Chaotic Modeling and Simulation (CMSIM) **4: 203-227, 2019**

Quantum Entanglement and Inflationary Cosmology Modeled by Nonlinear Lorentz Transformation

David C. Ni[1]

[1] Association of Industrial Technology Research Institute, Hsin Chu, Taiwan, R.O.C.
(E-mail: DavidNi@ alumni.itri.org.tw)

Abstract: Recent efforts on fusion of quantum entanglement and inflationary cosmology are propelled by new observatory data, such as 2015 Planck data sets, and motivated by prevailing unified theories, such as string theories. From application perspective, quantum computing and cryptography become potential implementations for large-scale ultra high-speed computing and communications. These emerging trends attract significant injections of scientific researches on the details and clarifications of the evolving theories in these two frontier fields.

In this work, we extend our efforts in modelling dark matter, dark energy, as well as formation of stellar structures for modelling phenomena in these two fields. The iterations of Nonlinear Lorentz Transformation (NLT) mapping in triplet momentum space on the complex plane model earlier stage after Big Bang, and show that the solution sets are with momentum values at several orders higher than normalized unity (i.e., light speed) for all nonlinear degrees, which hereby proposed to model the inflationary phase. For higher-than-degree-2 NLT mapping, the solution sets are converged and bounded within the unity disc on the complex plane after few steps of iteration, while the global part of NLT mapping with *degree = 2* showing the solution sets with the momentum values beyond the unity disc even under long-time evolution. This observation is proposed to model quantum entanglement, namely, the long distance coupling of quantum states is through interactions at speeds higher than light speed. The observations are in connection with our earlier proposals of quantum formalism related to global part of NLT formalism with *degree = 2*.

The Big-Bang singularity represents a composite NLT state of all nonlinear degrees, which not only induces inflationary phase, but also predictably forms large-scale structures at early stage of universe evolution. This prediction is just observed by ALMA recently that tens of elliptical galaxies formed about 10 billion ago.

In summary, the solution sets of global part of NLT mapping with *degree = 2* maintain high-than-light-speed distributions of momentum triplet at Big Bang to

Received: 3 October 2019 / Accepted: 30 October 2019

ISSN 2241-0503

inflationary era and beyond. Other NLT mappings contribute to normal energy transport as well as formation of cosmic structures as the current observations.

Keywords: Astrophysics Nonlinear Lorentz Transformation, momentum triplet, Quantum Entanglement, Inflationary Cosmology.

1 Introduction

Quantum entanglement has been attracting significant efforts in theoretical, experimental, and observational studies. Theoretical trends are along the fusion of general relativity and quantum formalism, and more recently string theories. The progressive advances in the spatiotemporal setting face a fundamental issue of addressing long-distance interaction, which was also encountered in gravity and general relativity. Accordingly, a conjectured connection between quantum entanglement and inflationary cosmolgy is one of viable approaches among others. However, quantum field responsible for the hypothetical inflation period in the very early universe has not been clarified. One of recent approaches is the inclusion of quantum entanglement with existing inflationary theories for fitting the observed data. In the area of observational progresses, 2015 Planck data sets have been motivating tests on different inflationary models, such as exponential inflationary potential, Starobinsky inflationary potential, and Hilltop inflationary potential. The efforts are the inclusion of quantum entanglement for the modifications of these convex potentials in order to prevent from being ruled out by Planck data sets [1,2,3].

More recent efforts on quantum computing and protocol for proving Bell violation of a Bell inequality are still in the setting of distinguishing quantum from classical formalism, or even try to surpass the limits of classical methods. In an experimental exploration recently, exciting observations has just been claimed in a demonstration of the violation of a Bell inequality within observed images. This experiment provides a significant milestone in both research and application [4].

In the area of inflationary cosmology, the model was originally proposed by Guth [5] to resolve several encountered problems of universe evolution. The main stream theories are in conjunction with Grand Unified Theories (GUT) of elementary particles in terms of symmetrical breakings and phase transitions at different energy scales to the formation stage of particle families [6]. This inflationary hypothesis solves numerous problems including its two original targets: the horizon problem and the flatness problem. The horizon problem is the observation that the universe would not have had time to organize its own large-scale homogeneity through various causes in the time available since the Big

Bang. The flatness problem is the observation that the spatial curvature of the universe appears to be evolved for ~10^{10} years in a metastable state instead of collapsing in on itself or expanding to complete emptiness on the scale of the Planck time (5.4×10^{-44} s). Both problems are solved by postulating that the highly disordered and volatile universe immediately after the Big-Bang singularity undergoes a period of rapid expansion, flattening out any curvature and flinging all matter and energy beyond a cosmic horizon. The expansion will cause the observable portion of the universe to appear nonempty despite the entire or at least a much larger portion of it being in a vacuum state and possessing tiny fluctuations in an otherwise perfectly smooth background.

These tiny fluctuations in quantum formalism are taken to be the seeds of cosmic structure. The colloquial explanation for this is that quantum fluctuations in the modes of the inflation field (the scalar field responsible for inflation) become frozen when the size of the cosmic horizon becomes comparable to the wavelength of each mode, creating tiny fluctuations in the background gravitational field, thus theorizing consequently nucleation points for galaxies and other cosmic structures. In this setting, inflation provides avenues to construct structure formation.

The main evidence for inflation comes from the cosmic microwave background (CMB), a nearly uniform thermal glow of the universe at a temperature of ~2 K, first discovered by accident and later studied in detail by the sky mapping experiment known as the Cosmic Background Explorer (COBE). In addition to revealing a nearly perfect blackbody spectrum, COBE also revealed tiny fluctuations in temperature, the signatures of the tiny fluctuations that led to structure formation in the early universe. Its resolution was too low, however, to compare with specific inflationary models.

While the inflationary hypothesis conceptually solves the horizon and flatness problems, its proposal for solving the problem of structure formation still leaves challenges such as what specifically is the physical mechanism by which quantum fluctuations in a scalar field are aggregated by inflation into eventual classical density fluctuations in the matter distribution of the post-inflationary universe. Several avenues for pursuing this question are proposed, and the answers given depend on the model in question and possibly even on one's interpretation of quantum formalism. Some authors go so far as to postulate a need for new physics to explain the transition, with an appeal to dynamic collapse models - in which

gravity or some other principle induces a real, unambiguous, dynamical collapse of a superposition into one of its constituent states, namely quantum-to-classical transition needed to account for cosmic structure formation. As examples of efforts, Campo and Parentani showed that quantum decoherence induced by nonlinearities in the evolution is an alternative [7] and Mazur and Heyl proposed nonlinear couplings between two particles for the transition [8]. However, there remains no consensus on the mechanism by which quantum fluctuations become classical density fluctuations during or after inflation.

From formalism-fusion perspective, the universe undergoes a homogeneous and isotropic expansion in spacetime in terms of Friedmann-Lemaître-Robertson-Walker (FLRW) metric. When the conformal symmetry is broken there is a net particle production due to the expansion of the universe. For both bosonic and fermionic fields, the generation of particles due to the expansion of the spacetime also generates entanglement in the final states of the field. These quantum correlations were shown to contain information about the expansion, enabling the possibility of deducing cosmological parameters of the underlying spacetime from this entanglement. However, in the conformal case, quantum entanglement is not generated by the expansion, on the other hand, it was present in the field to begin with and the effect of expansion on the swapping of this pre-existing field entanglement to local setting.

The efforts into the connection between cosmology and entanglement are vast, ranging from studies of entanglement in field modes, to the ability to swap this entanglement to local detectors, to the extraction of cosmological parameters from such measurements, to direct comparison of observational data and theoretical models, to the experimental probing of theoretical proposals in analogue experiments. Among these efforts, observational cosmology can now look for witnesses of purely quantum effects in the early universe. Other parallel efforts have arisen that uses laboratory analogues of expanding spacetime to study entanglement and reveals strong qualitative differences between the bosonic and fermionic entanglement generated by such expansion. The particular way in which fermionic fields get entangled encodes more information about the underlying spacetime than that of the corresponding bosonic case, thereby allowing reserchers to reconstruct the parameters of the history of the expansion more easily. This highlights the importance of bosonic/fermionic statistics to account for relativistic effects on the entanglement of quantum fields. This difference between fermions and bosons was already proven to be important in

other relevant phenomena in relativistic quantum information, such as entanglement in non-inertial frames, stationary black-holes, and stellar collapse scenarios [9]. In the newly engaged string theories, quantum entanglement and inflationary cosmology is connected to holography [10].

Howerver, the current theories and formalisms are not quite at positions to clarify the connections of (a) quantum fluctuations and Newtonian-relativistic mechanisms for formation of cosmic structures and (b) quantum entanglement and inflationary cosmology. Hereby we extend our NLT formalism in conjunction with triplet momentum space to explore these fuzzy zones.

2 NLT Mapping of Triplet Momentum Space

We have constructed a set of generalized Nonlinear Lorentz Transformation (NLT) in conjunction with momentum space (linear-angular-spin triplet) on the complex plane for N-body computation in the context of dynamical systems. The solution sets in the codomain on the complex plane are the convergent momentum-triplet sets mapped from the convergent momentum-triplet sets in the domain on the complex plane via iterations of NLT mapping, which representing time-evolution in the momentum space. NLT mapping is mathematically called as Blaschke products after German mathematician, W. Blaschke [11].

The solution sets, which generally follow the Fundamental Theorem of Algebra (FTA), manifest that this construction showing rich structures for modeling several challenging phenomena, such as dark matter, dark energy, formation of hierarchical stellar systems, phase transitions, even quantum formalism and so on in the area of cosmology and astrophysics as well as in other diciplines of physics.

These solution sets also show some canonical distributions, such as quasi-Gaussian distributions [18]. For proposing models for cosmic structures as well as clarifying the relationship between quantum entanglement and inflationary cosmology, we firstly review construction of NLT mapping, topological transitions, formation, and evolution of hierarchical systems in this section.

2.1 Construction

Given two inertial frames with different momentums, u and v, the observed momentum, u', from v-frame is as follows:

$$u' = (u - v) / (1 - vu/c^2) \quad (1)$$

We set $c^2 = 1$ and then multiply a global term, $exp(i\psi)$, where ψ is a real number, to the normalized complex form of the equation (1) to obtain the following equation:

$$u'/u = exp(i\psi)(1/u)[(u-v)/(1-uv)] \quad (2)$$

We hereby define a generalized complex function as follows:

$$f_{,}(z,m) = z^{-1} \Pi^m C_i \quad (3)$$

And C_i has the following form:

$$C_i = exp(i\psi)[(a_i-z)/(1-\bar{a}_i z)] \quad (4)$$

Where z is a complex variable representing the momentum u, a_i is a parameter representing momentum v, $\bar{a}_i$ is the complex conjugate of a complex number a_i and m is an integer. The degree of $f(z,m) = P(z)/Q(z)$ is defined as $Max\{deg\ P, deg\ Q\}$.

A domain can be the entire complex plane, C_∞, or a set of complex numbers, such as $z = x+yi$, with $(x^2 +y^2)^{1/2} \leqq R$, and R is a real number. For solving the NLT equation, a function f will be iterated as:

$$f^n(z) = f \circ f^{n-1}(z), \quad (5)$$

Where n is a positive integer defined as number of iteration. The function operates on a domain on the complex plane. The set of $f^n(z)$ is called mapped codomain or simply a codomain. In the figures, the regions in black color or other colors represent the convergent sets of the concerned equations and the white (i.e., blank) regions correspond to the divergent sets, the complementary sets of convergent sets on C_∞ as defined in dynamical systems [12-17].

The definition of triplet momentum space is shown in Fig. 1. On the complex plane, x-axes and y-axes are defined as normalized linear and angular momentum respectively. The local spin momentum is defined at individual point on the complex plane. The color plate shows several sets in differernt colors. Each set will map onto a corresponding set in the solution sets in the codoamin on the complex plane as shown in Fig. 1.

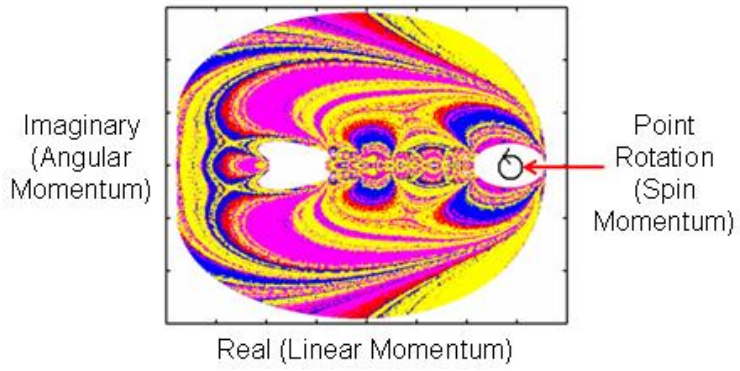

Fig. 1. Definition of linear-angular-spin triplet momentum space. Each color set in the domain on the complex plane will map onto individual solution set.

In order to characterize the convergent sets in the domain and codomain, we define a set of parameters called parameter space. The parameter space includes six parameters: (1) z (2) a (3) $exp(i\psi)$ (4) *iteration* (5) *degree* and (6) *rotation angle* θ. The parameter z represents an entity in momentum ensemble, and a is the momentum of reference frame. The rotation angle θ is defined in equation 6 below representing a local spin or rotation in momentum space, and $exp(i\psi)$ represents a global rotation with angle ψ in momentum space. The parameter *iteration* represents time evolution, and *degree* for nonlinearity.

$$a_\theta = a(\cos\theta + \sin\theta) \tag{6}$$

2.2 Topological Transitions

In addition to value mapping, Fig. 2 shows another mapping from the convergent sets of domain to codomain. This is a point-to-point mapping at same position between domain and codomain. The plots show absolute, real, and imaginary values respectively on the complex plane. The plot of imaginary values demonstrates conjugate symmetry to the y-axis, namely, the relationship of $z(-x, y) = -z(x, y)$ is defined as conjugate symmetry, which indicates a similar mechanism of Cooper pairs in superconductivity.

Fig. 3 shows topological transitions as value of $\{a\}$ increases from 0.55 to 0.65. The transition value (i.e., $a = 0.60$ in Fig. 3) depends on the *degree* (n) that as *degree* increases, the transition value increases [19,20].

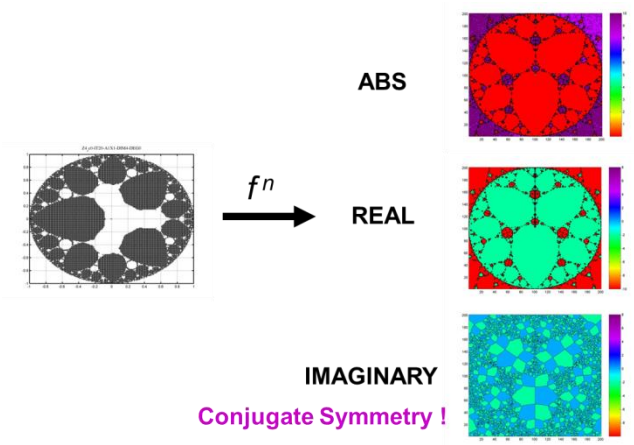

Fig. 2. Separation of Real and Imaginary values in Domains

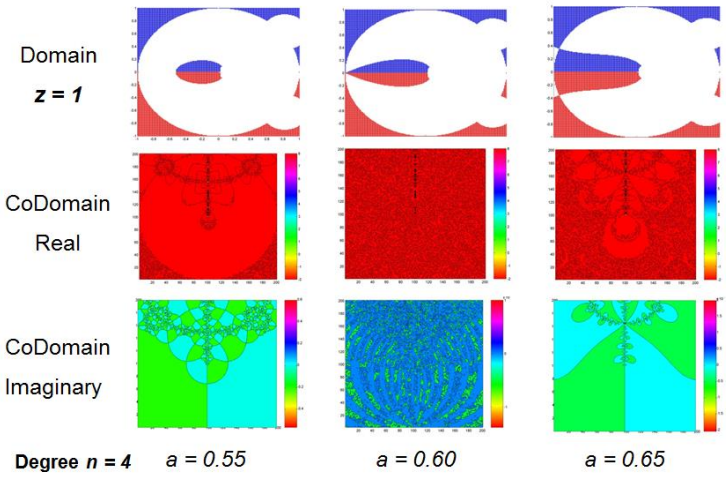

Fig. 3 Topological Transitions in Domain and Codomain

The topological transitions of NLT mapping show that this formalism provides a build-in characteristics similar to symmetrical breakings and phase transitions for modelling inflationary cosmology.

2.3 Hierarchical Structures

As specified in equation 7 below, the solution sets in the codomain as shown in Fig. 4(a), which are further expanded into Fig. 4(b) in a form of three clusters.

We then further expand the plot of three solution sets of Fig. 4(b) to three individual sub-plots, Cluster 1, 2, and 3 as shown in Fig. 5.

$$a_\theta = a\,(\cos(120*\pi/180) + \sin(120*\pi/180))\ \text{ with } degree = 3 \quad (7)$$

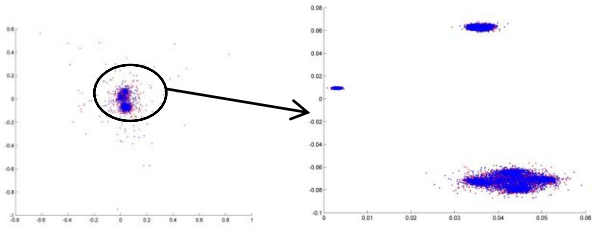

(a) Convergent sets in codomain (b) Expanded the circled area in (a)

Fig. 4. The distributions of the convergent sets for $a = 0.1$, $\theta=(120*\pi/180)$ and $degree = 3$ in the codomain.

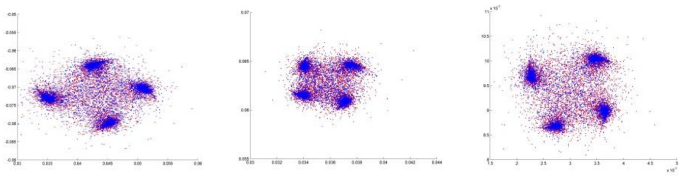

(a) Cluster 1 (b) Cluster 2 (c) Cluster 3

Fig. 5. The 1st-level expanded distributions of the convergent sets for $a = 0.1$, $\theta=(120*\pi/180)$ and $degree = 3$ in the codomain.

Each cluster contains four sub-clusters. Next, we select one of four sub-clusters in Cluster 1 as shown Fig. 5(a), and expand one more level (2nd level) down to show the solution sets as in Fig. 6. In contrast with $degree = 3$ case, $degree = 1$ or $degree = 2$, the solution sets do not form hierarchical structures.

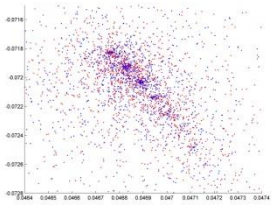

Fig. 6. The 2nd -level expanded distributions of the convergent sets for $a = 0.1$, $\theta=(120*\pi/180)$ and *degree* = *3* in the codomain.

Fig. 7(a) shows that for *degree* = *2*, when spin momentum $\theta = 0$, the solution sets in codomain shows two sets, which complies with Fundamental Theorem of Algebra (FTA). With spin momentum $\theta = 45$, the solution sets show discrete sets, which distribute randomly in the codomain as shown in Fig. 7(b). This is similar to energy levels in quantum formalism. As nonlinear degree increases higher than *degree* = *3*, the hierarchical structures will form at lower θ values.

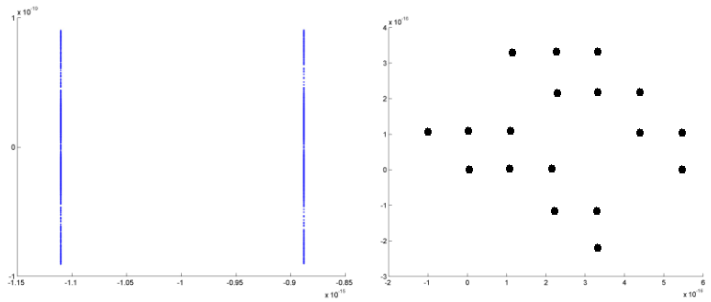

(a) $\theta = 0$ (b) $\theta = 45$

Fig. 7. For *degree* = *2*, (a) solution sets with spin momentum $\theta = 0$ (b) solution sets with spin momentum $\theta = 45$.

From perspectives of spatiotemporal modeling, we propose that the nonlinearity depends on different eras or stages of universe evolution. At so-proposed Big-Bang moment and following inflationary phase, the nonlinearity is at high degree composition, and as the universe expands, global nonlinearity becomes dominated by low-degree ones. As for *degree* = *1* or *degree* = *2*, we propose that modelling energy transportation by *degree* = *1* mechanism and long-distance interactions by *degree* = *2* mechanisms.

2.4 Evolution of Hierarchical Structures

Fig. 8 shows the scales of normalized momentums in the codomain expand from a 10^{-16} *through* 10^{-1} as the hierarchical structures evolve and become null set. This indicates that as spin momentum increases, total momentums also increase, and the universe will also expand in spatiotemporal perspectives [21,22,23].

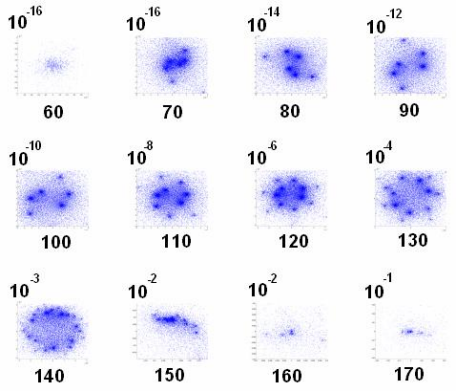

Fig. 8. Solution sets with *values of θ (60 through 170) and corresponding scales of momentum(10^{-16} through 10^{-1})* in *a (cos θ+ i*sinθ)* with *degree = 4 and a = 0.1*

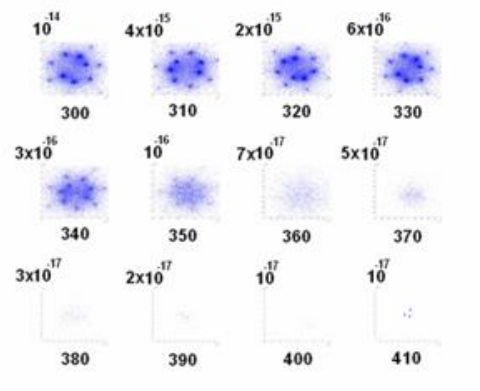

Fig. 9. Solution sets with *values of iteration (300 through 410) and corresponding scales of momentum (10^{-14} through 10^{-17})* in *a (cos θ+ i*sinθ)* with *degree = 4 and a = 0.1*

On the contrary, the parameter: *iteration*, which is defined as time evolution in section 2.1, demonstrates contraction of momentum triplet. Fig. 9 shows that as values of *iteration* increases from *300* to *410*, the momentum values contract and eventually become fixed-point solution sets, which are proposed to model black holes. In this conjunction, the NLT mapping demonstrates the effects of gravity. Further efforts are in the computational calibration of momentum-iteration and spatiotemporal evolution for gravitational law [24,25].

3 Momentum conversation and mass-energy conversion

Before further investigating on long-distance interactions, we examine closely the conversation laws regarding to momentum and mass-energy conversion.

3.1 Conversation Laws

As described in the previous section, the solution sets become null set as spin momentum exceeds some critical values or in a specific zones. This indicates that conversation laws are broken. Nonlinear interactions among momentum triplet are expected to result in exchange and dissipation of individual momentum values. To investigate these characteristic values, we define the following quantities [26]:

(a) Linear momentum (L): Summation of linear momentum of solution sets.
(b) Angular momentum (A): Summation of angular momentum of solution sets.
(c) Total momentum (T) is the square root of summations of squares of linear and angular momentum of solution sets, namely, T = *sqrt* (L^2 + A^2).
(d) Count of all points represents total mass in the solution sets.
(e) Local Spin momentum angle θ in [$a\ (\cos\theta + i*\sin\theta)$]
(f) Global rotation reference angle [$exp(\psi)$]

Fig. 10 shows logarithmic values of total momentum versus θ of spin momentum. Particularly, we examine the *degree = 3* (blue arrow) and *degree = 4* (red arrow) cases.

The next step is to examine the time evolutions of the particular zones of local spin in the context of conversation laws. For *degree = 4* case, we have one zone showing that outside the critical zone, total momentum does not change during time evolution (θ = *70* and θ = *110* in Fig. 11), while others showing non-conservative due to divergence.

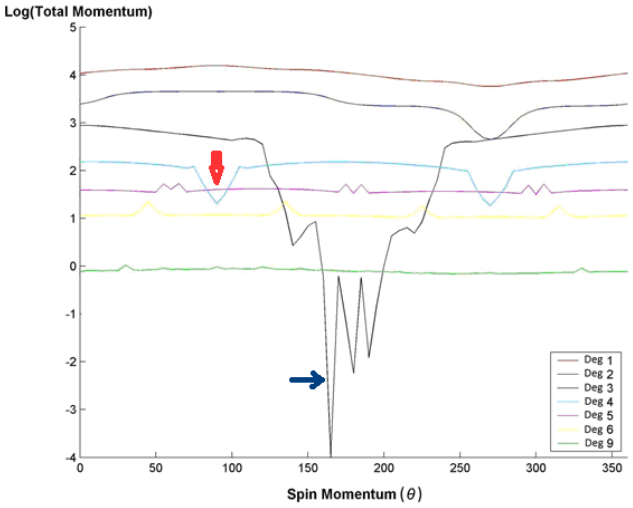

Fig. 10. log (T) vs. local θ values of local spin momentum *(0 through 360)* for nonlinear *degree= 1* through *9*. Blue arrow points to the critical zone of *degree = 3*, and red arrow points to one of critical zones of *degree = 4*.

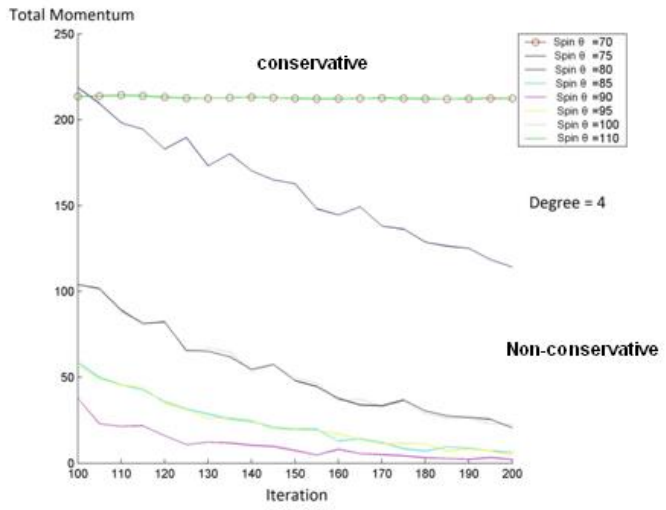

Fig. 11. Total momentum vs. iteration (100 through 200) showing non-conservative inside critical zone (θ *=75* through θ *=110*)

3.2 Global and Local rotations

As specified in the previous section, we further examine local spin versus global rotation with nonlinear degrees. Fig. 12 shows linear, angular, and total momentums in green, red, and blue color for *degree = 1*. Both plots show sinusoidal patterns. Both linear and total momentums are symmetrical toψ*=180 or* θ*=180* plane, while the angular momentums shows symmetrical to the point (*180,0*). The total momentums are conservative through iterations [21,22].

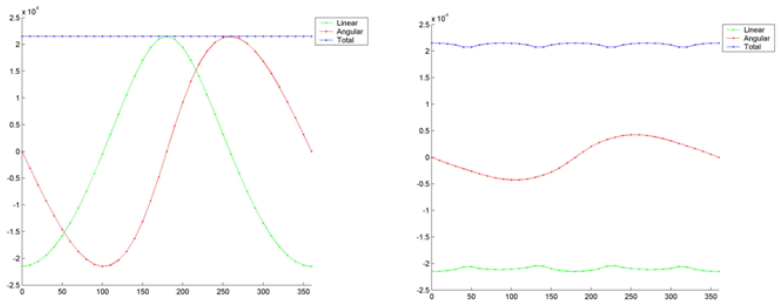

(a) Global (b) Local

Fig. 12. Momentum Triplet vs. rotation angles (*0* through *360*)
Linear (Green) Angular (Red) and Total (Blue)
(a) Global (b) Local for nonlinear *degree = 1*.

Fig. 13 shows linear, angular, and total momentums in green, red, and blue color for *degree = 2*. The local plot, Fig. 13(b), shows harmonic compositions of sinusoidal patterns, while the global plot, Fig. 13(a), shows different patterns. The global plot includes one critical zone (ψ*=30* toψ*=330*), while local plot does not have critical zone. Symmetries are similar to *degree = 1* plots.

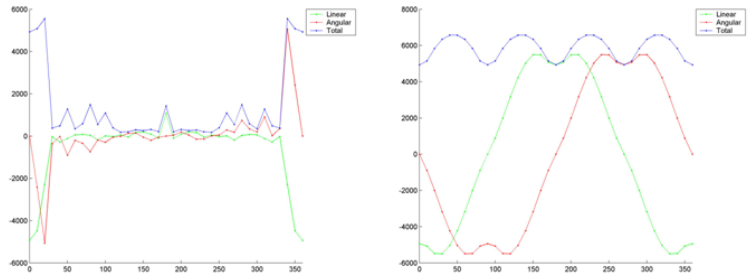

(a) Global (b) Local

Fig. 13. Momentum Triplet vs. rotation angles (*0* through *360*)
Linear (Green) Angular (Red) and Total (Blue)
(a) Global (b) Local for nonlinear *degree = 2*.

Fig. 14 shows linear, angular, and total momentums in green, red, and blue color for *degree = 3*. Both global and local plots show similar patterns with one critical zone (Ref. Fig. 10), where conservation laws broken. Symmetries are similar to *degree = 1* plots.

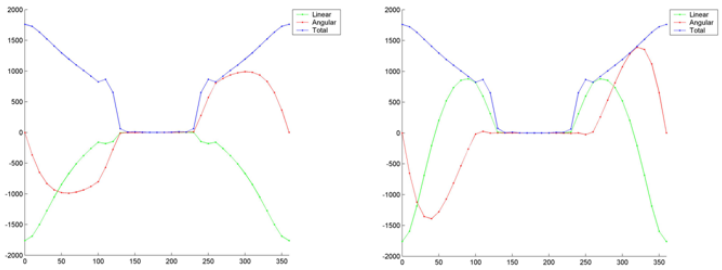

(a) Global (b) Local

Fig. 14. Momentum Triplet vs. rotation angles (*0* through *360*)
Linear (Green) Angular (Red) and Total (Blue)
(a) Global (b) Local for nonlinear *degree = 3*.

Fig. 15 shows linear, angular, and total momentums in green, red, and blue color for *degree = 4*. The global plot shows with one critical zone, while the local plot shows two critical zones. Symmetries are similar to *degree = 1* plots.

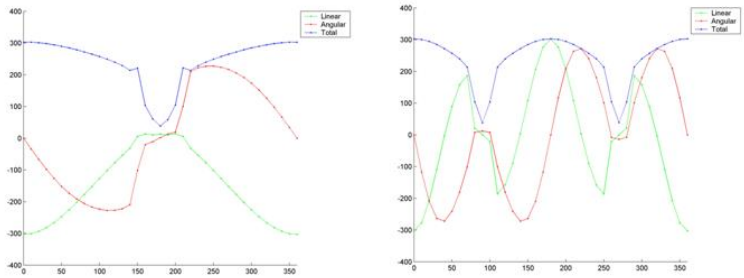

(a) Global (b) Local

Fig. 15. Momentum Triplet vs. rotation angles (*0* through *360*)
Linear (Green) Angular (Red) and Total (Blue)
(a) Global (b) Local for nonlinear *degree = 4*.

Fig. 16 shows linear, angular, and total momentums in green, red, and blue color for *degree = 5*. The global plot shows with one critical zone, while the local plot shows three critical zones. The shapes of critical zones are different from *degree = 3* and *degree = 4*. Symmetries are similar to *degree = 1* plots.

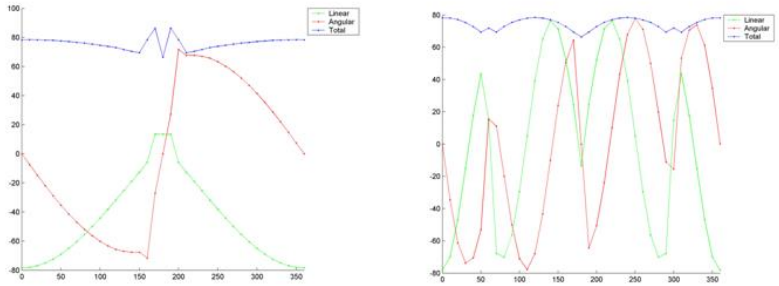

(a) Global (b) Local

Fig. 16. Momentum Triplet vs. rotation angles (*0* through *360*)
Linear (Green) Angular (Red) and Total (Blue)
(a) Global (b) Local for nonlinear *degree = 5*.

Fig. 17 shows linear, angular, and total momentums in green, red, and blue color for *degree = 5*. The global plot shows with one critical zone, while the local plot shows four critical zones. The shapes of critical zones are different from *degree = 3* and *degree = 4*, nevertheless, similar to the plot of *degree = 5*. More preciously, the critical zones in the plots of *degree = 5* reflects a transition from the plots of *degree = 3* and *degree = 4 to degree = 6*. This shape indicates increases of total momentums, which will be discussed in the next section regarding to mass-energy conversion. Symmetries are similar to *degree = 1* plots.

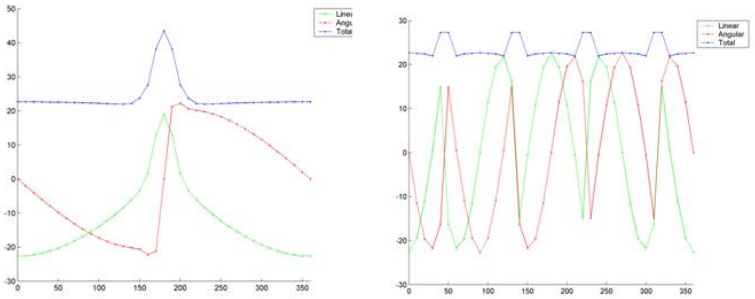

(a) Global (b) Local

Fig. 17. Momentum Triplet vs. rotation angles (*0* through *360*)
Linear (Green) Angular (Red) and Total (Blue)
(a) Global (b) Local for nonlinear *degree = 6*.

As the nonlinear degree increases, the number of critical zone in global plot keeps as one, while number of critical zone of local plot increases as *degree – 2*. Also,

the shapes of critical zone start to change from *degree = 5* and show increases of total momentums instead of reductions as in *degree = 2* (global plot), *degree = 3*, and *degree = 4*.

3.3 Mass and energy conversion

The plots of momentum triplet versus rotation angle in previous section show some areas in or at edges of critical zones where the total momentums increase. We can further examine the plot of momentum triplet versus iteration as shown in Fig. 11.

Fig. 18 (a) shows that when the count of all points in the solution sets in green color, which indirectly represents system mass (Section 3.1d). As the value of *iteration* increases from *1* to *200*, the count decreases around *iteration = 50*, *110*, and *160*, where higher count reduction rates observed, the total momentums as well as linear and angular momentums (Fig. 18(b)) are sharply increase. Comparing with the plot in Fig. 11, we propose that mass-energy conversion manifests at higher nonlinear degrees with value greater than 4.

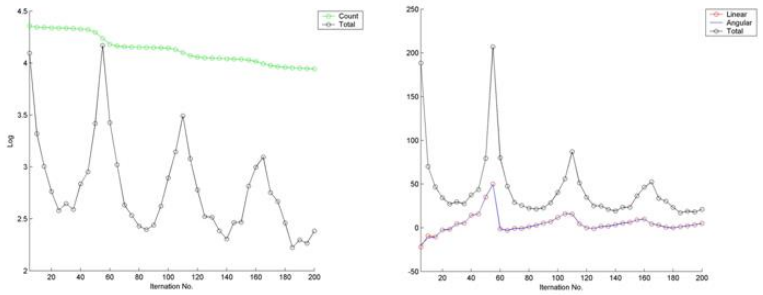

(a) count -total momentum vs. iteration (b) momentum triplet vs. iteration

Fig. 18. Count-Momentum vs. iteration (*1* through *200*) for nonlinear *degree = 6*. (a) Count (Green) and Total momentum (Black)
(b) Linear (Red) Angular (Blue) and Total momentum (Black)

Nevertheless, we can also observe mass-energy conversion at lower degrees, particularly in global rotation at *degree = 2* as shown in Fig. 19 (Ref. Fig. 13(a)).

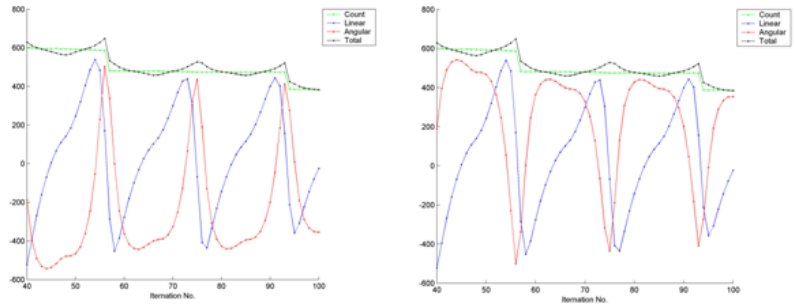

(a) count-momentum vs. iteration (b) count-momentum vs. iteration

Fig. 19. Count-Momentum vs. iteration (*40* through *100*)
for nonlinear *degree = 2*.
(a) at global rotation $\psi = 30$ (b) at global rotation $\psi = 330$

Fig. 19(a) shows the count (green color) reduces in quantized steps, where both linear (blue color) and angular (red color) momentums surge and result in the spiky shapes of total momentums (black color). Symmetric to $\psi = 180$, the angular momentums show at positive values at $\psi = 30$, while negative values at $\psi = 330$.

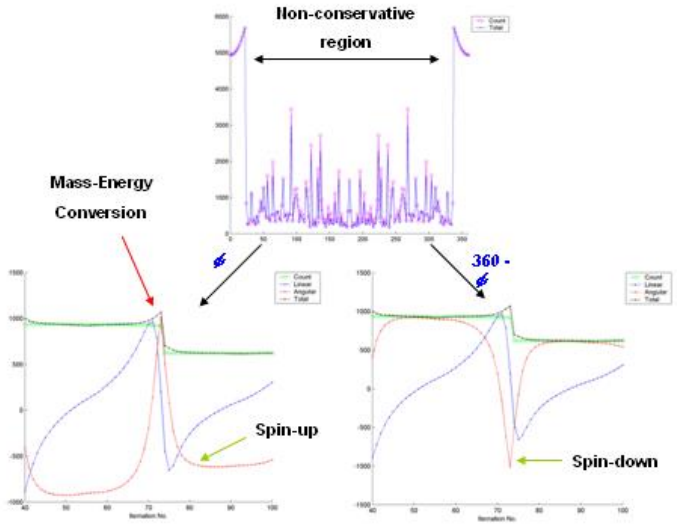

Fig. 20. Count-Momentum vs. iteration (*40* through *100*) for nonlinear *degree = 2*. Two plots at bottom are at ψ and $360 - \psi$ respectively. The angular momentums are at positive and negative values correspondingly.

We hereby to propose that this observation, as shown in Fig. 20, provide reference so-called spin-up and spin-down solution of Dirac equation. Inside the non-

conservative zone of *degree = 2* global-rotation plot, the point count of solution sets shows mass-energy conversion and the angular momentums show one positive and the other negative value symmetrical to $\psi = 180$. Combining with random mapping [24], we propose that a strong connection between quantum formalism and NLT with *degree = 2* mapping. We will extend this perspective to quantum entanglement in the next section.

4 Inflationary Cosmology and Quantum Entanglement

As discussions in section 1, current efforts for fusion of inflationary cosmology and quantum entanglement are in the connections of quantum and classical mechanisms for modeling formation of cosmic structures and in the clarifications of interactions between quantum entanglement and inflationary cosmology. Along this line, we firstly extend NLT formalism in the structual fromation and explore the relationship between quantum formalism and NLT formalism as in the previous sections. In this section, we continue to use the methodologies, namely momentum triplet and time evoluion via iteration, for the interaction clarifications. Accordingly, we proceed to examine NLT formalism in the very early universe via time evolution for different nonlinear degrees in the context of connections of quantum and NLT formalisms.

4.1 Models

As presented in section 2 through 3, we have constructed this NLT formalism to explore an alternative approach to formation of cosmic structure in the context of nonlinearity instead of being induced from quantum fluctuations. As proposed, we justify that quantum formalism is potentially represented by *degree = 2* mapping of NLT formalism, while structure formation is modeled by *degree = 3* or higher nonlinearity. For investigating on the relationship of inflationary theories and quantum entanglement, we further examine time evolution via *iteration* as shown in section 3 on the early universe. Given the age of our universe is commonly accepted about 13.8 billion years, we estimate that each iteration represents approximately a period of 10^6 years of time evolution, therefore this approach may not be able to approach to Planck time scale, nevetheless, the results of first iteration shall reveal valuable information of our targeting subjects. Table 1 below shows normalized scales of total momentums of the global rotation and local spin as defined in section 3.1. The distributions of total momentums are the values over all possible rotation or spin angles as shown in Fig. 12 through Fig. 17.

CoDomain	Scale	Iteration = 1	Iteration = 20	Iteration = 50	Iteration = 100
Degree = 1	**Global Rotation**	**10**	**1.E-11**	**1.E-15**	**1.E-15**
	Local Spin	**10**	**1.E-11**	**1.E-15**	**1.E-15**
Degree = 2	**Global Rotation**	**10**	**10**	**10**	**10**
	Local Spin	**10**	**10**	**1.E-09**	**1.E-15**
Degree = 3	**Global Rotation**	**10**	**10**	**10**	**1**
	Local Spin	**10**	**10**	**10**	**1**
Degree = 4	**Global Rotation**	**10**	**10**	**1**	**1**
	Local Spin	**10**	**10**	**1**	**1**
Degree = 5	**Global Rotation**	**10**	**10**	**1**	**1**
	Local Spin	**10**	**10**	**1**	**1**
Degree = 20	**Global Rotation**	**10000**	**1**	**0.002**	**0.001**
	Local Spin	**10000**	**0.1**	**0.005**	**0.004**
Degree = 50	**Global Rotation**	**4.00E+08**	**5.00E-01**	**1.00E-03**	**3.00E-04**
	Local Spin	**1.50E+19**	**4.00E-02**	**3.00E-02**	**2.00E-04**

Table 1. Normalized scales of distributions of total momentums vs. iteration number

As shown in Table 1, depending on nonlinear degrees, the distributions of total momentums of global rotation and local spin are several orders higher than normalized unity momentum at first iteration, when the universe is about 10^6 years old after Big Bang. As the iteration value increases to *50* and the distribution of momentums falls in a small zone of momentum space for both global and local cases of nonlinear *degree = 1*.

For the *degree = 2*, the distributions of total momentums show similar evolutions of local case as that *degree = 1*. For the global case, the momentum distribution keeps as one order higher than unity even iteration value increases to *100*. We propose that this is a candidate for the mechanism of quantum entanglement. This feature combines with others, such as random mapping and quantized mass-energy conversion, further support our proposal that quantum formalism is closely linked to global case of NLT formalism with *degree = 2*. But the observation indicates that quantum entanglement is not a by-product of inflationary cosmology, which is rather a composite phenomenon of overall-

degree nonlinearity at singularity. We can further manifest this viewpoint when examine the time evolutions of NLT mapping in conjunction with low iteration numbers, which represent the early universe stage in the next section.

For the *degree = 3*, *4*, and *5* as shown, we observe that the distributions of total momentums will be confined in the unity disc of momentum space when iteration number is equal to *100* for both global and local cases. As nonlinear degrees become larger, the initial iterations show much higher values of total momentums than unity. As examples, the last four rows in Table 1 show several orders higher than unity for the cases of nonlinear *degree = 20* and *degree = 50*. This high order values, such as 4 orders of *degree = 20* is quite fitting to an earlier experiment result [27]. We are hereby to propose that experiments for verifying quantum entanglement are subject to nonlinear environments, such as in the vicinities of the black holes. On the other hand, the values of total momentums will also converge faster than low-degree ones as shown for *iteration = 20*, *50*, and *100*. The composite degrees will certainly provide reasonable interpretation of the mechanism of inflationary cosmology.

Based on the simulations, the NLT formalism provides very comprehensive models for both inflationary cosmology and quantum entanglement. During Planck time period just after Big Bang, the singularity provides tremendous composite nonlinearity, which therein produces unpredictable momentums to induce inflationary phase. As the domain scale of universe increases, the high-degree nonlinearity then proceeds to nucleate bosons and fermions. The low-degree nonlinear momentums, particularly NLT mapping with *degree = 2*, which maintains conformal interactions as quantum entanglement.

4.2 Formation of Cosmic Structures in Early Universe

Recent ALMA observations show that formation of tens of large-scale elliptical galaxies formed about 10 billion ago in the early ears of universe, which are not well fitted to the existing models [28]. We hereby proceed to model this observation by NLT formalism. Fig. 21 shows some solution sets of low iteration numbers for *degree = 4*. For the first iteration, the solution sets distributed in the zone of x-axis range (-3,3) and y-axis range (-3,3) as shown in Fig. 21(a) (the scales are labeled onto coordinates). For the second iteration, the solution sets are in the unity disc as shown in Fig. 21(b). Further expanding the range internal subsets of the unity disc in Fig 21(b) as shown in Fig. 21(c) with *iteration = 2*, we observe that two aggregated sets, which representing hierarchical structures

since there are substructures after further expansion. The third iteration results in Fig. 21(d), which shows additional aggregated set forms. Subsequently, the three-set configuration will merge to two-set configuration as show in Fig. 21(e) for *iteration = 4*, Fig. 21(f) for *iteration = 5*, and Fig. 21(g) for *iteration = 10*. Eventually, the solution sets will contract to one set in this coordinate range as shown in Fig. 21(h), which is similar to the demonstration in Fig. 9.

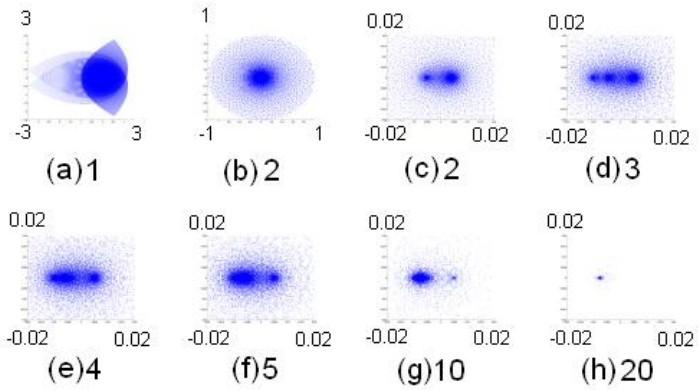

Fig. 21. Solution sets vs. iterations for nonlinear *degree = 4*.
(a) *iteration = 1* (b) *iteration = 2* (c) *iteration = 2* (d) *iteration = 3*
(e) *iteration = 4* (f) *iteration = 5* (g) *iteration = 10* (h) *iteration = 20*

For this demonstration of modeling structure formation in the early Universe, we have not engaged local spin momentums. The structural sets form symmetrically to the x-axis, and the total angular momentums are null. Again, for *degree = 1* and *degree = 2*, we can't produce hierarchical structures either at low iteration numbers.

In summary, NLT formalism provides rather straightforward and comprehensive methodologies to model some complicated observations as well as to clarify the relationship between inflationary cosmology and quantum entanglement, which are very challenging in spatiotemporal setting. We are currently working on the connections between this NLT formalism and general relativity in the context of specific sets of composite nonlinearities to the corresponding definitions of metric theories.

5 Remarks

In this paper, we present the construction of momentum triplet, namely linear, angular, and spin momentums, on the complex plane, which represents all momentums of an N-body system, in conjunction with Nonlinear Lorentz Transformation (NLT), which maps the convergent domain of momentum triplet on the complex plane onto the codomain of momentum triplet on the complex plane. We have obtained the solution sets, which comply with Fundamental Theorem of Algebra (FTA). Violations of FTA are also allocated in the regions of topological transitions of solution sets.

Instead of modeling in spatiotemporal setting, this formalism is proposed to model some challenging physical phenomena in momentum space, such as dark matters, dark energy, formation of hierarchical stellar systems, quantum formalism, phase-topological transitions and so on. We proceed further to examine the conversation laws of the NLT formalism and model mass-energy conversion. By doing so, we have identified that NLT formalism with nonlinear *degree = 2* is well mapped to quantum formalism. However, this *degree = 2* mapping has not enough nonlinearity to form cosmic structures in this triplet momentum simulation setting.

For clarifying the current investigations on inflationary cosmology and quantum entanglement, we examine the initial time evolution of individual degrees through iteration of mapping. During Planck time period after Big Bang, the singularity provides enough composite nonlinearity for producing tremendous momentums, which induce inflationary phase. As the domain scale of universe evolves, the high-degree nonlinearity consequently forms cosmic structures even in early universe. The low-degree nonlinear momentums, particularly NLT mapping with *degree = 2*, which maintains conformal interactions as quantum entanglement.

Acknowledgement

Firstly, we would like to express my sincere respect to Prof. Christos H. Skiadas for his cordial and continuous orchestration of the worldwide activities and publications of CMSIM communities.

For local activities in Asia Pacific regions, we appreciate the members of Gravity Society of Republic of China (GSROC) for the encouragement of studies in new frontiers and coordination of conferences and workshops for different levels of the scholars and students in physics.

References

1. E. D. Valentino and L. Mersini-Houghton. Testing Predictions of the Quantum Landscape Multiverse 2: The Exponential Inflationary Potential *arXiv:1612.08334v1*, Dec 26, 2016.
2. E. D. Valentino and L. Mersini-Houghton. Testing Predictions of the Quantum Landscape Multiverse 1: The Starobinsky Inflationary Potential *arXiv:1612.09588v2*, Mar 6, 2017.
3. E. D. Valentino and L. Mersini-Houghton. Testing Predictions of the Quantum Landscape Multiverse 3: The Hilltop Inflationary Potential *arXiv:1807.10833v2* [astro-ph.CO] 10 Apr 2019.
4. P. A. Morris, M. J. Padgett, P-A Moreau, E. Toninelli, T. Gregory, R. S. Aspden. Imaging Bell-type nonlocal behavior, *Science Adv.*, May 2019, July 12, 2019
5. A. H. Guth. Inflationary universe: A possible solution to the horizon and flatness problems *Phys. Rev. D 23, 347*, 1981.
6. A. Linde. Particle Physics and Inflationary Cosmology, *arXiv:hep-th/0503203v1* 26 Mar 2005.
7. D. Campo and R. Parentani. Quantum Correlations in Inflationary Spectra and Violation of Bell Inequalities *Braz. J. Phys. 35, 1074*, 2005.
8. D. Mazur and J. S. Heyl. Characterizing entanglement entropy produced by nonlinear scalar interactions during inflation, *Phys. Rev. D 80, 023523*, 2009.
9. E. Martın-Martınez and N. C. Menicucci. Cosmological quantum entanglement *arXiv:1204.4918v2*, Oct. 19, 2012
10. S. Koh, J. H. Lee, C. Park and D. Ro. Quantum entanglement in inflationary cosmology *arXiv:1806.01092v1*, 4 Jun 2018
11. W. Blaschke, Eine Erweiterung des Satzes von Vitali. über Folgen analytischer Funktionen, *Berichte Math.-Phys. Kl., Sächs. Gesell. der Wiss*. Leipzig , No. 67, pp. 194–200, 1915.
12. D. C. Ni and C. H. Chin, $Z^{-1}C_1C_2C_3C_4$ System and Application, *Proceedings of TIENCS workshop*, Singapore, August 1-5, 2006.
13. D. C. Ni and C. H. Chin. Symmetry Broken in Low Dimensional N-body Chaos, *Proc. of Chaos 2009 Conference*, Chania, Crete, Greece, pp. 53, June 1-5, 2009.
14. D. C. Ni and C. H. Chin. Symmetry Broken in low dimensional N-Body Chaos, *CHAOTIC SYSTEMS: Theory and Applications* (ed. by C. H. Skisdas and I. Domotikalis), pp. 215-223, 2010
15. D. C. Ni. Chaotic Behaviour Related to Potential Energy and Velocity in N-Body Systems, *Proceedings of 8th AIMS International Conference on Dynamical Systems, Differential Equations and Applications*, May 25-28, 2010, Dresden, Germany, pp. 328.
16. D. C. Ni and C. H. Chin. Classification on Herman Rings of Extended Blaschke Equations, *Differential Equations and Control processes, Issue No. 2, Article 1*, 2010.
17. D. C. Ni. Numerical Studies of Lorentz Transformation, *Proceeding of 7th EASIAM*, Kitakyushu, Japan, June 27-29, 2011, pp. 113-114.
18. D. C. Ni. Statistics constructed from N-body systems, *Proceeding of World Congress, Statistics and Probability*, Istanbul, Turkey, July 9-14, 2012, pp. 171.
19. D. C. Ni. Phase Transition Models based on A N-Body Complex Statistics, *Proceedings of the World Congress on Engineering 2013 (WCE 2013)*, Vol I, pp. 319-323, London, UK, July 3 - 5, 2013.

20. D. C. Ni. A Counter Example of Fundamental Theorem of Algebra: ExtendedBlaschke Mapping, *Proceedings of ICM 2014*, August 13-21, Seoul, Korea, 2014.
21. D. C. Ni. Chaos in Complex and Quaternion Blaschke Maps, *Chaos 2018*, June 5 – 8, Rome, Italy.
22. D. C. Ni. Quaternion Maps of Blaschke Products, *International Congress of Mathematics 2018 (ICM 2018)*, Rio de Janeiro, Brazil, August 1-9, 2018
23. D. C. Ni. Formation of hierarchical stellar systems modelled by Momentum on Complex plane in conjunction with Nonlinear Relativity, *The Eighth East Asian Numerical Astrophysics Meeting (EANAM 2018)*, October 22-26, 2018, National Cheng-Kung University (NCKU), Tainan, Taiwan, R.O.C.
24. D. C. Ni. Modelling Formation of Stellar Systems, Dark Matter, and Dark Energy with Nonlinear Special Relativity, *TPS 2019,* Jan. 23–25, 2019, NCTU, Hsin Chu, Taiwan, R.O.C.
25. D. C. Ni. Modeling Formation of Stellar Systems, Dark Matter, and Dark Energy with Nonlinear Special Relativity, *YITP 2019*, Feb. 11–15, 2019, YITP, Kyoto University, Kyoto, Japan
26. D. C. Ni. Relativistic Quantum formalism constructed by Nonlinear Lorentz Transformation, *RQI-N 2019,* May 27 – June 1, 2019, NCKU, Tainan, Taiwan, R.O.C.
27. D. Salart, A. Baas, C. Branciard, N. Gisin, and H. Zbinden. Testing spooky action at a distance, *arXiv:0808.3316v1* [quant-ph] 25 Aug 25, 2008
28. https://www.almaobservatory.org/en/press-release/alma-identified-dark-ancestors-of-massive-elliptical-galaxies/